# Solid State Reaction Study of the System Li<sub>2</sub>CO<sub>3</sub>/Fe<sub>2</sub>O<sub>3</sub>

V. Berbenni, A. Marini, and D. Capsoni

C.S.G.I., e Dipartimento di Chimica Fisica dell'Università di Pavia – Viale Taramelli, 16, 27100 Pavia – Italy

Z. Naturforsch. 53a, 997-1003 (1998); received November 19, 1998

A thermoanalytical (TGA/DSC) and diffractometric (XRD) study has been performed on the solid state reaction system  $\rm Li_2CO_3$ –Fe<sub>2</sub>O<sub>3</sub> in the  $x_{\rm Li}$  range 0.10÷0.50. A detailed analysis of the results shows that the data are in agreement with a reaction model where the carbonate decomposition is regulated by the formation of both LiFe<sub>5</sub>O<sub>8</sub>, and the relative amount of the two phases depends on the initial composition. The DSC evidence offers the possibility to directly quantify the LiFe<sub>5</sub>O<sub>8</sub> phase. Furthermore it allows one to obtain the enthalpies of formation of both LiFeO<sub>2</sub> and LiFe<sub>5</sub>O<sub>8</sub>.

Key words: Lithium Ferrites; Solid State Reaction; Iron (III) Oxide; Lithium Carbonate; TGA; DSC.

#### 1. Introduction

The  $\alpha$ -Fe<sub>2</sub>O<sub>3</sub>/Li<sub>2</sub>O system has received considerable attention since lithium ferrite (LiFe<sub>5</sub>O<sub>8</sub>), one of the phases of the system, has found technological application because of its square loop properties coupled with good thermal stability [1-3]. Several papers have appeared concerning the electrical and magnetic properties of lithium ferrites [4]. Also the crystal structures of the different phases have been studied [5, 6], as well as the electrochemical insertion of lithium oxide into iron (III) oxide [7-9]. Furthermore, the structure and physical properties of lithium ferrites have been studied on samples prepared by different methods, such as ionic exchange in molten systems [10], hydrothermal methods [11] and precipitation from Fe(III) solutions [12]. Attention has been payed also to the thermal stability of the LiFeO<sub>2</sub> phase in relation to the effect of lithium and oxygen losses on its magnetic and crystallographic properties [2].

A concerns the formation reaction of lithium ferrites and the solid state, a paper was published [13], dealing with the system Li<sub>2</sub>CO<sub>3</sub>/Fe<sub>2</sub>O<sub>3</sub>, in which, however, only the molar compositions 1:1 and 1:2 were analysed. In the present work we intend, starting from the same reacting system, to perform a solid state reaction study in a wider composition range by means of thermoanalytical techniques (TGA, DSC) and X-ray powder diffraction (XRD).

### 2. Experimental

#### 2.1. Products and Sample Preparation

Iron (III) Oxide and lithium carbonate powders were obtained from Aldrich Chimica (Italy) and Merck (Italy) respectively. Lithium carbonate was characterised both by thermogravimetric analysis and X-ray diffraction. The TGA curves showed only a mass loss due to the release of carbon dioxide (640 °C<T<800 °C). All the reflections of the XRD patterns were attributable to Li<sub>2</sub>CO<sub>3</sub>. On the contrary iron oxide showed, besides the  $\alpha$ -Fe<sub>2</sub>O<sub>3</sub> (hematite) reflections, the presence of some Fe<sub>3</sub>O<sub>4</sub> spinel phase (magnetite) (see Fig. 1a). It has however to be noted that no presence of the spinel phase was detected after the commercial iron oxide was heated up to 850 °C (see Fig. 1b).

Mixtures of the starting products (about 1 g) were prepared by weighing the appropriate amounts of the two components and dry mixing them in an agate mortar for 20 minutes. The composition range was  $x_{Li}$  (lithium cationic fraction) =  $0.10 \div 0.50$ . All the sample mixtures were then heated in the TGA and DSC apparatuses to obtain the final samples. In two cases ( $x_{Li} = 0.167$ , corresponding to LiFe<sub>5</sub>O<sub>8</sub> composition, and  $x_{Li} = 0.500$  corresponding to LiFeO<sub>2</sub> composition) samples were also prepared by heating the pertinent mixtures (about 3 g) in a horizontal tube furnace (Stanton Redcroft, maximum operating temperature 1700 °C) under the same experimental conditions as in TGA.

Reprint requests to: Prof. A. Marini; E-mail: marini@matsci. unipv.it

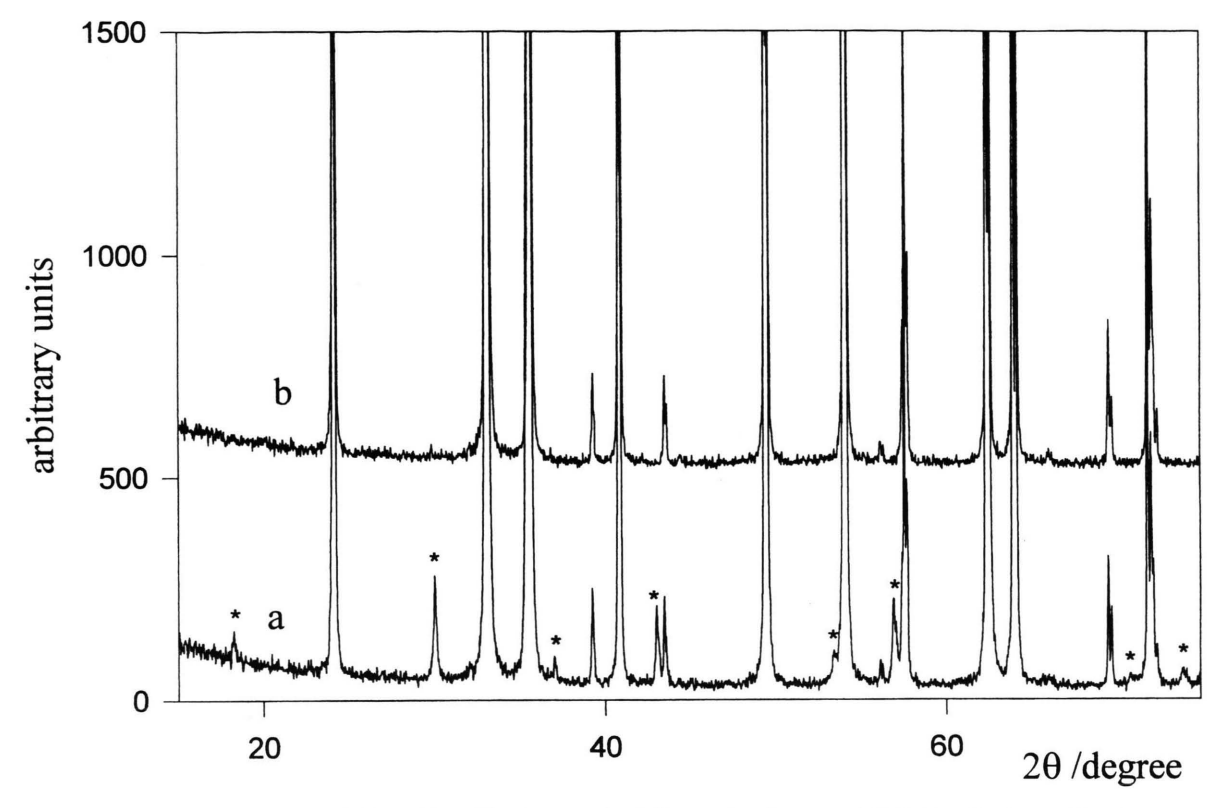


Fig. 1. XRD patterns of commercial iron(III) oxide. a) as received; b) after heating up to 850 °C. \* reflexions of Fe<sub>3</sub>O<sub>4</sub>.

#### 2.2. Apparatus and Procedures

## 2.2.1. TGA Measurements

TGA measurements were performed by the thermogravimetric analysers TA Instruments Mod. 2950 and DuPont 951. TA 3100 and TA 2000 Data Analysis Systems (with proprietary software) were respectively connected to the two TGA modules. The sample mixtures were heated under a flow of air +10% by volume of  $\rm CO_2$  (100 ml min<sup>-1</sup>) at 2 °C min<sup>-1</sup> between room temperature (rt) and 850 °C. An isothermal period of 12 hours followed the heating ramp.

#### 2.2.2. DSC Measurements

DSC measurements were accomplished by a high temperature DSC (Stanton Redcroft Mod. 1500, maximum operating temperature 1500 °C, alumina sample cups). Data were acquired and analysed by a Rheometric Scientific Data Station. The sample mixtures were heated under the same dynamic atmosphere used in thermogravimetric experiments, while the heating rate was 5 °C

min<sup>-1</sup> and the samples were heated up to 900 °C. No isothermal stage followed the heating ramp.

# 2.2.3. XRD Measurements

Diffraction data were obtained by a Philips PW1710 powder diffractometer equipped with a Philips PW1050 vertical goniometer. Use was made of the  $\text{CuK}\alpha$  radiation monochromatized by a graphite bent crystal monochromator. The patterns were collected in the angular region  $14-130^\circ$  in step scan mode (0.03°/step, 3 s counting time/step). Due to the very limited amount (ca. 20 mg) of TGA samples available, the powders were dispersed with some droplets of acetone on a single crystal slide of silicon.

#### 3. Results and Discussion

### 3.1. $Fe_2O_3$ Sample

As noted in the experimental section, the original commercial iron (III) oxide contains some  $Fe_3O_4$ . To try and

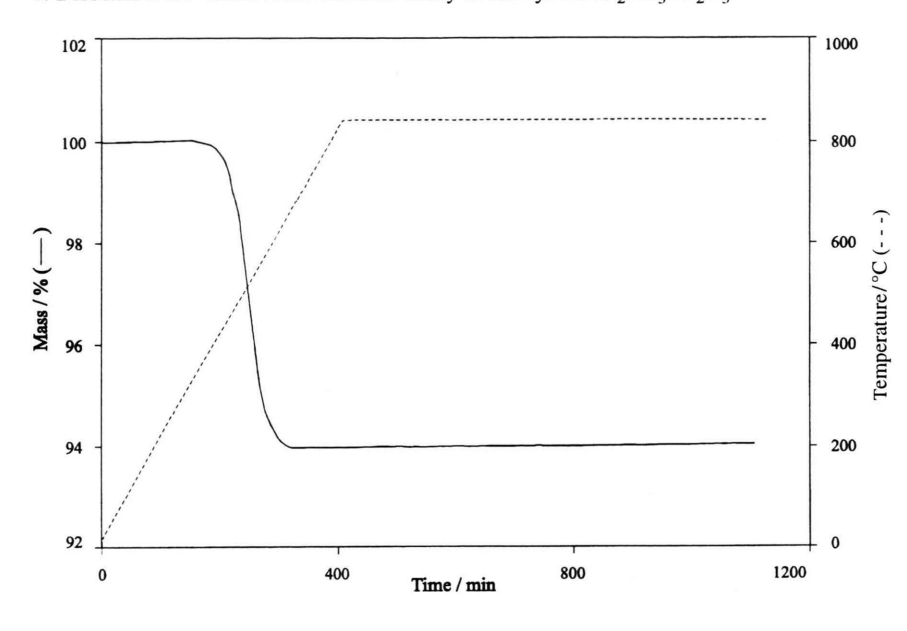


Fig. 2. TGA run of a  $x_{Li} = 0.201$  mixture. Full line: weight data; broken line: temperature data.

Table 1. Experimental ( $\Delta M_{\text{tot}}$ ) and calculated ( $\Delta M_{\text{I}}$ ) mass loss values (see text).

$x_{\text{Li}} \Delta M_{\text{tot}}$ (%)	0.101	0.170	0.201	0.250	0.297	0.343	0.425	0.500
	-2.94	-5.09	-6.07	-7.96	-9.73	-11.52	-15.05	-18.72
$\Delta M_{\rm I}(\%)$	-2.76	-4.99	-6.05	-7.80	-9.59	-11.45	-15.05	-18.73

assess the content of such a phase, TGA runs were performed. Also in these experiments the samples were heated up to 850 °C and kept at this temperature for 12 hours. From several runs the mean weight gain of  $\pm 0.196 \pm 0.004\%$  was obtained, which is due to the oxidation of the Fe<sub>3</sub>O<sub>4</sub> phase present in our iron oxide commercial sample. The reaction can be represented as follows:

$$(1-\alpha) \cdot \operatorname{Fe}_{3} O_{4} + \alpha \cdot \operatorname{Fe}_{2} O_{3} + \frac{(1-\alpha)}{4} \cdot O_{2} \rightarrow \frac{(3-\alpha)}{2} \cdot \operatorname{Fe}_{2} O_{3}$$

were  $\alpha$  represents the molar fraction of Fe<sub>2</sub>O<sub>3</sub> (hematite) in our commercial sample. We note that, here and in the following, the reaction equations will be written using stoichiometric coefficients deduced from the chemical composition of the system under study. With these coefficients, therefore, it is straightforward to calculate the percentage mass change associated to the reaction. In the case of Fe<sub>3</sub>O<sub>4</sub> oxidation, it should be;

$$\Delta M (\%) = 0.196 = \frac{\frac{(1-\alpha)}{4} M_{\text{O}_2}}{(1-\alpha) M_{\text{Fe}_3\text{O}_4} + \alpha M_{\text{Fe}_2\text{O}_3}} \cdot 100$$

where the symbol M represents the relevant molar mass. Solving for  $\alpha$  one obtains  $\alpha = 0.960$  which corresponds to 5.70% w/w of Fe<sub>3</sub>O<sub>4</sub> phase in the commercial sample. Such an amount is in a fair agreement with that found by XRD (Rietveld refinement).

# 3.2. $Li_2CO_3/Fe_2O_3$ Mixtures

#### 3.2.1. TGA Measurements

Figure 2 reports the TGA curve obtained on the  $x_{\rm Li}$  = 0.201 mixture. The trend of the curve is representative of the mixtures in the entire composition range. It can be seen that the mass loss process due to Li<sub>2</sub>CO<sub>3</sub> decomposition starts at about 400 °C, indicating that the decomposition process is regulated by the formation of lithium ferrite(s). Such a temperature is indeed sensibly lower than that of spontaneous Li<sub>2</sub>CO<sub>3</sub> decomposition ( $\approx$  640 °C). Table 1 reports the results of the TGA measurements performed on all the mixtures. According to the XRD results (see the following section), and assuming that all Fe(II) contained in Fe<sub>3</sub>O<sub>4</sub> oxidizes to Fe(III) and that stoichiometric products are obtained, the reactive process can be represented as follows:

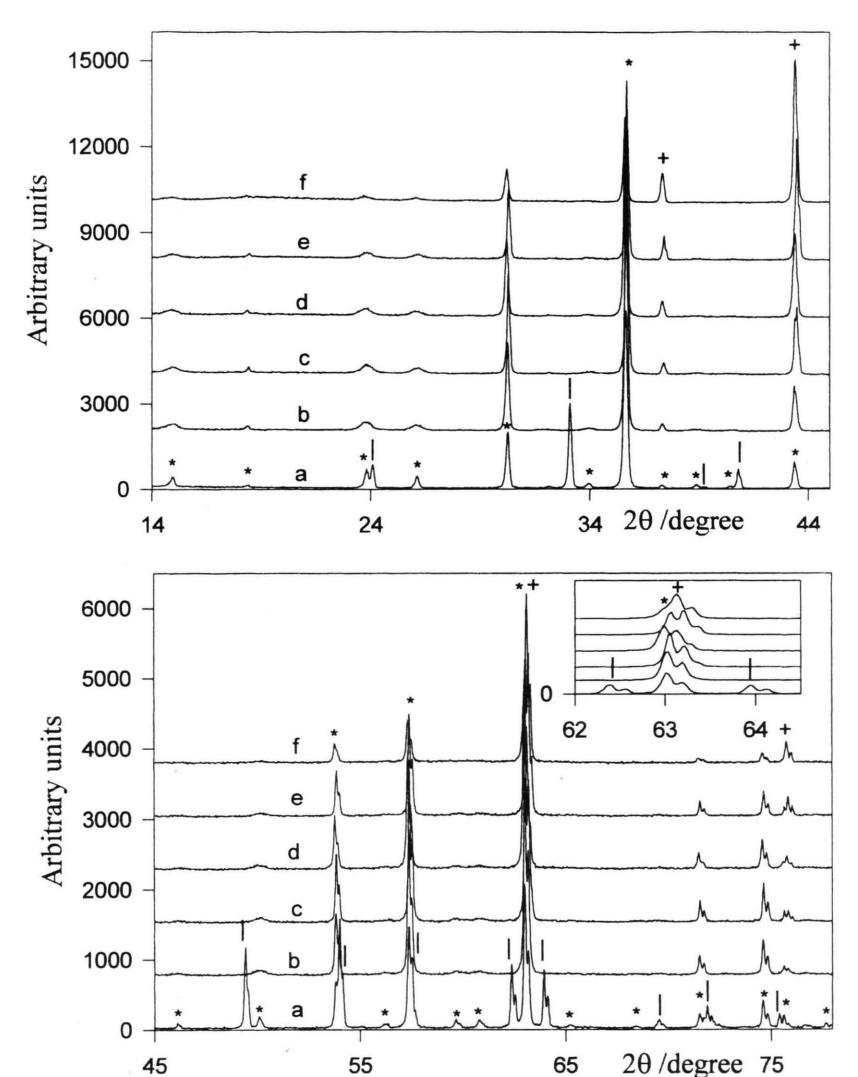


Fig. 3. XRD patterns of samples recovered after TGA measurements: a)  $x_{\text{Li}} = 0.101$ ; b)  $x_{\text{Li}} = 0.201$ ; c)  $x_{\text{Li}} = 0.250$ ; d)  $x_{\text{Li}} = 0.297$ ; e)  $x_{\text{Li}} = 0.343$ ; f)  $x_{\text{Li}} = 0.425$ . l: Fe<sub>2</sub>O<sub>3</sub>; \* LiFe<sub>5</sub>O<sub>8</sub>; +: LiFeO<sub>2</sub>

$$\begin{split} \frac{x_{Li}}{2} \cdot Li_2CO_3 + \frac{(1 - x_{Li}) \cdot 8}{17} \cdot Fe_2O_3 + \frac{(1 - \alpha) \cdot (1 - x_{Li}) \cdot 8}{17 \cdot \alpha} \cdot Fe_3O_4 + \frac{(1 - \alpha) \cdot (1 - x_{Li}) \cdot 2}{17 \cdot \alpha} \cdot O_2 \to \\ \frac{2}{17} \cdot \left[ \frac{(77 \cdot x_{Li} + 8)}{8} - \frac{3 \cdot (1 - x_{Li})}{\alpha} \right] \cdot \text{LiFeO}_2 + \frac{2}{17} \cdot \left[ \frac{3 \cdot (1 - x_{Li})}{\alpha} - \frac{1}{8} \cdot (9 \cdot x_{Li} + 8) \right] \cdot \text{LiFe}_5O_8 + \frac{x_{Li}}{2} \cdot \text{CO}_2 \,. \end{split}$$

Table 1 also reports the percentage mass losses calculated  $(\Delta M_1)$  according to this reaction scheme, in which the mass loss due to Li<sub>2</sub>CO<sub>3</sub> decomposition is partially compensated by a small oxygen intake from the atmosphere. It can be seen that the experimental mass losses  $(\Delta M_{\text{tot}})$  are in quite good agreement with the expected ones  $(\Delta M_1)$ .

#### 3.2.2. XRD Measurements

In Fig. 3 the XRD spectra collected on all the reacted mixtures are reported. From the XRD data analysis the following considerations can be proposed:

i) the Fe<sub>2</sub>O<sub>3</sub> reflections are present only in the  $x_{Li} = 0.101$  sample, where there is excess of iron oxide with

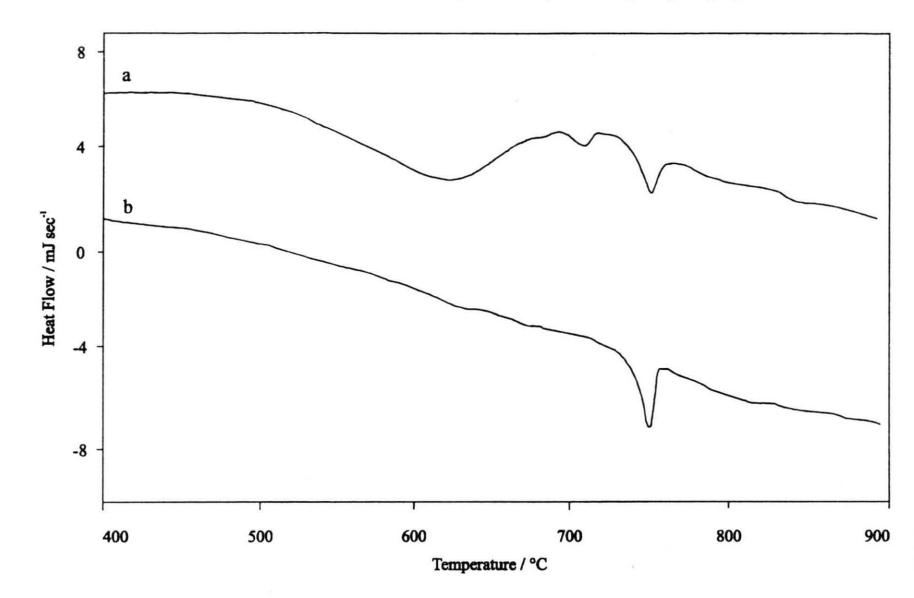


Fig. 4. DSC curve of: a)  $x_{Li} = 0.201$  mixture; b) pure LiFe<sub>5</sub>O<sub>8</sub>.

respect to the stoichiometric composition of the lower lithium ferrite. Their absence in mixtures with higher lithium content ( $x_{Li} > 0.170$ ) confirms (see the TGA results) that there was quantitative formation of the ferrite phases in all samples;

ii) for samples with  $x_{\rm Li} > 0.201$ , the peaks belonging both to the LiFeO<sub>2</sub> and LiFe<sub>5</sub>O<sub>8</sub> phases can be observed. Due to the strong overlapping of the LiFeO<sub>2</sub> reflections with some of the LiFe<sub>5</sub>O<sub>8</sub> ones (both compounds have a cubic structure with a = 4.158 Å [17 938 JCPDS card] and a = 8.337 Å [17 115 JCPDS card], respectively), it is difficult to assess the relative abundances of the two phases. However it can be seen in Fig. 3 that, with increasing  $x_{\rm Li}$ , the reflection intensities of the LiFe<sub>5</sub>O<sub>8</sub> phase show a definite tendency to decrease, while those of LiFeO<sub>2</sub> increase. Such a trend is better visible at high diffraction angles (see inset of Fig. 3), where enhanced peaks separation for overlapping reflections is to be expected;

iii) some LiFe<sub>5</sub>O<sub>8</sub> reflections become rather broad. This is not surprising if we take into account that the two phases present, besides showing the peaks closely overlapped, have their peculiar microstructure that affects the peak broadening. Moreover the peak broadening in LiFe<sub>5</sub>O<sub>8</sub> (spinel type structure) is no doubt affected also by its degree of disorder.

In general, the XRD measurements show that the solid state reaction is completed in all mixtures and that it leads to the formation of both the LiFeO<sub>2</sub> and LiFe<sub>5</sub>O<sub>8</sub> form. Moreover, the XRD measurements show an oppo-

site trend of the relative abundances of the two phases with respect to  $x_{Li}$ ; namely the LiFeO<sub>2</sub> phase increases with increasing  $x_{Li}$  while the LiFe<sub>5</sub>O<sub>8</sub> one decreases.

#### 3.2.3. DSC Measurements

Figure 4a reports the DSC curve of the  $x_{\rm Li} = 0.201$  mixture between ca. 400 and 900 °C. Such a thermal trace is representative of all the analysed mixtures. The features of this thermal curve are a wide endothermic hump starting at about 480 °C, a sharp endothermic peak ( $T_{\rm max}$  ca. 710 °C) which suddenly emerges from the hump and, after the hump is over, an endothermic peak ( $T_{\rm max}$  ca. 755 °C). While the sharp peak at ca. 710 °C is likely due to some extent of spontaneous carbonate decomposition (as its area increases with  $x_{\rm Li}$ \*), that at ca. 755 °C is characteristic of the LiFe<sub>5</sub>O<sub>8</sub> phase. Indeed, such a phase was prepared by firing the appropriate amounts of the components in a tubular furnace (see Experimental Section). The DSC scan of pure LiFe<sub>5</sub>O<sub>8</sub> showed only the 755 °C peak with an enthalpy of 18.08 J g<sup>-1</sup> (see Fig. 4b).

The DSC data are reported in Table 2. It can be seen that even in the case of the  $x_{\rm Li} = 0.170$  mixture, the area of the peak at about 755 °C ( $\Delta H_{\rm LiFe_5O_8}$ ) is considerably lower than that found in the case of the sample with the same nominal composition but prepared by furnace treatment (and constituted, according to XRD evidence, by

<sup>\*</sup> Incidentally it can be noted that a strictly similar behaviour was observed in the case of the solid state system Ni/Li<sub>2</sub>CO<sub>3</sub> [14].

0.101 0.201 0.250 0.297 0.343 0.500  $\Delta_{\text{tot}}^{X_{\text{Li}}}H/J \text{ g}^{-1}$   $\Delta H_{\text{LiFe}_5\text{O}_8}/J \text{ g}^{-1}$ 0.170 0.425 188.95 81.30 117.03 150.52 204.64 265.47 360.48 476.79 12.48 11.74 11.96 9.89 7.43 3.69

Table 2. DSC data.  $\Delta_{\text{tot}}H$  is the wide hump area.  $\Delta H_{\text{LiFe}_2O_8}$  is the 755 °C peak area.

pure LiFe<sub>5</sub>O<sub>8</sub>). This should not be surprising, if allowance is made of the different thermal schedule adopted in the furnace treatment (2 °C min<sup>-1</sup> up to 850 °C+12 h isothermal stage) and in the DSC scan (ramp at 5 °C min<sup>-1</sup> up to 900 °C): the combination of a higher heating rate and the absence of an isothermal stage at  $T_{\rm max}$  leads to a lower conversion extent in DSC experiments. Such a conclusion is confirmed by XRD, which shows the presence of both LiFe<sub>5</sub>O<sub>8</sub> and Fe<sub>2</sub>O<sub>3</sub> in the sample recovered after DSC treatment.

Calculating the conversion extent by the experimental (12.48  $\cdot$  Jg $_{mix}^{-1}$ ) and reference (18.08  $\cdot$  Jg $_{LiFe_5O_8}^{-1}$ ) enthalpy values, and referring to such a conversion degree the enthalpy change due to the reaction (117.03 Jg $_{mix}^{-1}$ ), one obtains

$$117.03 \cdot Jg_{\text{mix}}^{-1} \cdot \frac{18.08 \cdot Jg_{\text{LiFe}_5O_8}^{-1}}{12.48 \cdot Jg_{\text{mix}}^{-1}}$$
$$= 169.5 \cdot Jg_{\text{LiFe}_5O_8}^{-1} \equiv \Delta_{1/5}H,$$

where  $\Delta_{1/2}H$  represents the enthalpy of the reaction

$$\begin{aligned} \text{Li}_2\text{CO}_3(s) + 4.706 \cdot \text{Fe}_2\text{O}_3(s) + 0.196 \cdot \text{Fe}_3\text{O}_4(s) \\ + 0.0491 \cdot \text{O}_2(g) &\rightarrow 2 \cdot \text{LiFe}_5\text{O}_8(s) \\ + \text{CO}_2(g). \end{aligned}$$

On the other hand, as concerns the  $x_{Li} = 0.500$  mixture we have to consider the reaction

$$\text{Li}_2\text{CO}_3(s) + 0.941 \cdot \text{Fe}_2\text{O}_3(s) + 0.0392 \cdot \text{Fe}_3\text{O}_4(s) + 0.0098 \cdot \text{O}_2 \rightarrow 2 \cdot \text{LiFeO}_2(s) + \text{CO}_2(g).$$

In this case we should have (see Table 2 for the experimental value)

$$476.79 \cdot Jg_{mix}^{-1} = \Delta_{1/1} H \cdot Jg_{LiFeO_2}^{-1} \cdot \frac{g_{LiFeO_2}}{g_{mix}}.$$

The XRD analysis shows that the powders recovered after the DSC experiment contain LiFeO<sub>2</sub> only. Thus, as the reaction yield is known, the enthalpic change associated with the reaction can be easily obtained.

$$\Delta_{1/5}H = 586.7 \cdot Jg_{LiFeO_2}^{-1}$$

Once the  $\Delta_{1/1}H$  and  $\Delta_{1/5}H$  enthalpy values are known, an estimate of the relative amounts of LiFeO<sub>2</sub> and LiFe<sub>5</sub>O<sub>8</sub>

Table 3. Amounts of LiFeO<sub>2</sub> and LiFe<sub>5</sub>O<sub>8</sub> phases that would form according to DSC and TGA data (see text).

x <sub>Li</sub>	$m_{ m LiFeO_2/g}$ TGA	$m_{\rm LiFeO_2/g}$ DSC	$m_{\text{LiFe}_5\text{O}_8/g}$ TGA	$m_{\text{LiFe}_5\text{O}_8}/g$ DSC
0.201	6.97	6.90	86.96	64.93
0.250	17.84	13.09	74.20	66.15
0.297	28.28	19.08	61.99	54.70
0.343	38.88	33.38	49.60	41.09
0.425	59.68	55.54	25.27	20.41

can be performed as follows: From the  $\Delta H_{\rm LiFe_5O_8}$  values the amount of the LiFe<sub>5</sub>O<sub>8</sub> phase present in the different mixtures can be directly calculated. Then, the amount of LiFeO<sub>2</sub> formed at each composition can be calculated from the relationship

$$\frac{\Delta_{\frac{1}{1}} H \cdot g_{LiFeO_2} + \Delta_{\frac{1}{1}} H \cdot g_{LiFe_5O_8}}{g_{\text{mix}}} = \Delta_{\text{tot}} H \cdot Jg_{\text{mix}}^{-1}.$$

Table 3 reports the amounts (m/g) of the two phases calculated according to the described procedure (DSC, incomplete reaction). Also reported, for the sake of comparison, are the amounts of the same phases calculated according to the TGA data and the reaction scheme proposed (complete reaction). It can be seen that both the DSC and TGA predictions confirm the trend revealed by XRD: LiFeO<sub>2</sub> increases while LiFe<sub>5</sub>O<sub>8</sub> decreases with increasing  $x_{Li}$ . Moreover, the DSC predictions are generally lower than the TGA ones. This is expected and, as already observed, is due to the different experimental conditions adopted in TGA and DSC measurements (incomplete product formation in DSC). However it must be noted that both for  $x_{Li} = 0.201$  and  $x_{Li} = 0.425$  mixtures (i.e. for compositions near to the stoichiometry of the two ferrite phases), the DSC predictions for the LiFeO<sub>2</sub> phase are in good agreement with the TGA ones, while those for LiFe<sub>5</sub>O<sub>8</sub> are appreciably lower. This suggests that at both extremes LiFeO<sub>2</sub> forms more rapidly than LiFe<sub>5</sub>O<sub>8</sub>.

#### 4. Conclusions

The solid state reaction system  $\text{Li}_2\text{CO}_3/\text{Fe}_2\text{O}_3$  has been studied in the  $x_{\text{Li}} = 0.10 - 0.50$  composition range both

by thermal (TGA, DSC) and diffractometric (XRD) methods. The collected experimental evidence suggests the following conclusions:

- i) the Li<sub>2</sub>CO<sub>3</sub> decomposition starts well below its usual temperature so that it can be said that the LiFeO<sub>2</sub>/LiFe<sub>5</sub>O<sub>8</sub> formation is the step regulating the Li<sub>2</sub>CO<sub>3</sub> decomposition;
- ii) both LiFeO<sub>2</sub> and LiFe<sub>5</sub>O<sub>8</sub> form simultaneously, and the formation rate seems higher for the phase with the
- lower molar reaction enthalpy (LiFeO<sub>2</sub>). Anyway, the relative amount of the two ferrite phases at the end of the reaction is fundamentally determined by the composition of the starting mixture, so that it can be reliably predicted according to the reaction scheme proposed;
- iii) both LiFeO<sub>2</sub> and LiFe<sub>5</sub>O<sub>8</sub> can be obtained in a pure form by solid state reaction of mixtures with the relevant stoichiometric composition.
- [1] A. J. Pointon and R. C. Saull, J. Amer. Ceram. Soc. 52, 157 (1969).
- [2] D. H. Ridgeley, H. Lessof, and J. D. Childress, J. Amer. Ceram. Soc. 53, 304 (1970).
- [3] Yu D. Tretyakov, N. N. Oleinikov, Yu G. Metlin, and A. P. Erastova, J. Solid State Chem. 5, 191 (1972).
- [4] See for example: N. Ramachandran and A. B. Biswas, J. Solid State Chem. 30, 61 (1979); T. Esaka and M. Greenblatt, J. Solid State Chem. 71, 164 (1987).
- [5] S. J. Marin, M. O'Keeffe, and D. E. Partin, J. Solid State Chem. 113, 413 (1994).
- [6] M. Pernet, P. Strobel, B. Bonnet, P. Bordet, and Y. Chabre, Solid State Ionics 66, 259 (1993).
- [7] M. S. Islam and C. R. A. Catlow, J. Solid State Chem, 77, 180 (1988).
- [8] C. J. Chen and M. Greenblatt, Solid State Ionics 18/19, 838 (1986).

- [9] M. M. Thackeray, W. I. F. David, and J. B. Goodenough, J. Solid State Chem. 55, 280 (1984).
- [10] T. Shirane, R. Kanno, Y. Kawamoto, Y. Takeda, M. Takano, T. Kamiyama, and F. Izumi, Solid State Ionics 79, 227 (1995).
- [11] M. Tabuchi, K. Ado, H. Sakaebe, C. Masquelier, H. Ka-geyama, and O. Nakamura, Solid State Ionics 79, 220 (1995).
- [12] C. Barriga, V. Barron, R. Gancedo, M. Gracia, J. Morales, J. L. Tirado, and J. Torrent, J. Solid State Chem. 77, 132 (1988).
- [13] G. A. El-Shokabi and A. A. Ibrahim, Thermochim. Acta 118, 151 (1987).
- [14] A. Marini, V. Berbenni, V. Massarotti, G. Flor, R. Riccardi, and M. Leonini, Solid State Ionics, 32/33, 398 (1989).